ChemComm

Accepted Manuscript

This article can be cited before page numbers have been issued, to do this please use: D. Hursan, A. Kormanyos, K. Rajeshwar and C. Janaky, *Chem. Commun.*, 2016, DOI: 10.1039/C6CC04050K.

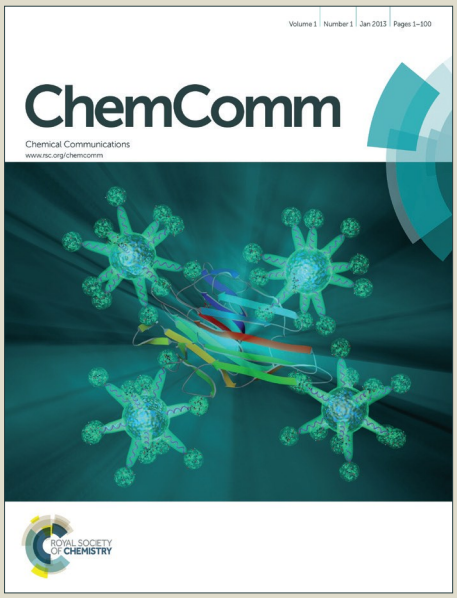

ROYAL SOCIETY OF CHEMISTRY

www.rsc.org/chemcomm

ROYAL SOCIETY OF CHEMISTRY View Article Online
DOI: 10.1039/C6CC04050K

Chemical Communications

COMMUNICATION

Polyaniline Films Photoelectrochemically Reduce CO_2 to Alcohols

Dorottya Hursán,[a,b] Attila Kormányos,[a,b,c] Krishnan Rajeshwar,*[c,d] and Csaba Janáky*[a,b]

Received 00th January 20xx,
Accepted 00th January 20xx

DOI: 10.1039/x0xx00000x

www.rsc.org/

In this Communication, we demonstrate that polyaniline, as the very first example of an organic semiconductor, is a promising photocathode material for the conversion of carbon dioxide (CO_2) to alcohol fuels. CO_2 is a greenhouse gas; thus using solar energy to convert CO_2 to transportation fuel (such as methanol or ethanol) is a value-added approach to simultaneous generation of alternative fuels and environmental remediation of carbon emissions. Insights into its unique behavior are presented from photoelectrochemical measurements and adsorption studies, together with spectroscopic data. Through a comparative study involving various conducting polymers, a set of criteria is developed for an organic semiconductor to function as a photocathode for solar fuel generation from CO_2.

The Sunlight is undoubtedly one of the most valuable resources in the quest for a diversified and sustainable energy supply.[1,2] Photoelectrochemistry has proven to be a promising, albeit, challenging avenue for solar water splitting[3]. Solar splitting of CO_2, however, is even more kinetically daunting, and requires the use of carefully designed photocathode surfaces to accelerate electron transfer rates to levels that make practical sense in terms of the overall energy balance[4,5]. A wide range of inorganic *p*-type semiconductors (SCs) (e.g., Si, CdTe, InP, GaAs, GaP, FeS_2, ZnTe, Cu_2O, and $CuFeO_2$[2,6–12] have been employed for photoelectrochemically reducing CO_2 either directly at the SC/electrolyte interface, or indirectly, employing a redox mediator[13]. At the same time, the use of an *inorganic* SC (with optoelectronically-acceptable properties) often necessitates the use of relatively high temperatures for its synthesis/processing and consequently, long energy payback time. Organic SCs are attractive from this perspective since they can be synthesized and processed via mild (low-temperature) routes; consequently, their energy payback time is much shorter. In this Communication, we show that polyaniline (PANI), a prominent member of the organic conducting polymer family, is eminently attractive as a photocathode material for CO_2 reduction. Importantly our proof-of-concept data below show that: (a) No co-catalyst is needed for sustaining the photoconversion to alcohol products; and (b) PANI shows the requisite surface selectivity for chemical interactions with CO_2. Interestingly, the findings of the present study would be in line with the fact that *N*-rich organic polymers (e.g., polyimines) are currently among the best solid-state adsorbents for CO_2[14–16]. Furthermore, conducting polymers such as polypyrrole (PPy) and PANI have shown *electro*catalytic activity towards CO_2 reduction[17,18]. These polymers have also been deployed in conjunction with inorganic SCs such as Si[19] and ZnTe[20] for the photoelectrochemical (PEC) reduction of CO_2. Conducting polymer-based hybrid organic photocathodes showed unprecedentedly high photocurrents, and high rates of PEC H_2-generation with the use of a (homogeneous) co-catalyst[21] in addition water oxidation was also demonstrated employing a special ladder-type conjugated polymer.[22] Finally, *N*-containing heterocycles such as pyridine[11,23] have been shown to be effective co-catalysts for the PEC reduction of CO_2 when used with SCs such as *p*-GaP.

The photovoltammograms presented in Fig. 1 bear all the hallmarks associated with the behavior of a *p*-type SC[24]. The photocurrents are cathodic in polarity, originating from the reduction of either H^+ ions or CO_2 at the conducting polymer/electrolyte interface. Photoexcitation of an electron from the valence band to the conduction band (via UV or visible light irradiation) is followed by electric-field separated photoelectrons being driven to the surface of the *p*-type SC where they can react with solution-confined species such as protons or CO_2.

[a] Department of Physical Chemistry and Materials Science, University of Szeged, Szeged, Hungary.
[b] MTA-SZTE „Lendület" Photoelectrochemistry Research Group, Rerrich Square 1, 6720, Szeged, Hungary.
[c] Department of Chemistry and Biochemistry, University of Texas at Arlington, Arlington, Texas, USA.
[d] Center for Renewable Energy Science & Technology, University of Texas at Arlington, Arlington, Texas, USA.

† Footnotes relating to the title and/or authors should appear here.
Electronic Supplementary Information (ESI) available: [details of any supplementary information available should be included here]. See DOI: 10.1039/x0xx00000x

View Article Online
DOI: 10.1039/C6CC04050K

Chemical Communications

COMMUNICATION

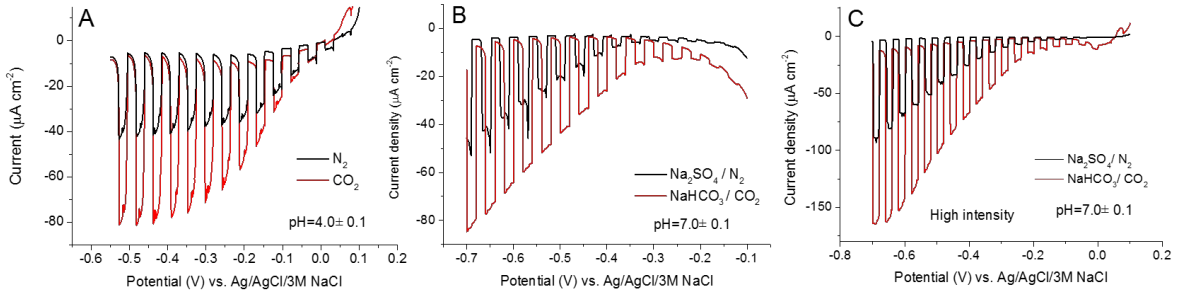

Fig. 1. Representative photocurrent-potential profiles for an electrodeposited PANI layer under chopped UV-vis illumination (Xe-Hg Arc lamp, 100 W output) in (A) N_2- and CO_2-saturated 0.1 M Na_2SO_4 aqueous solution where the N_2-saturated solution was buffered to pH = 4.0; (B) N_2- saturated 0.1 M Na_2SO_4 and CO_2-saturated $NaHCO_3$ aqueous solutions (pH = 7.0); (C) photocurrent-potential profiles of an electrodeposited PANI layer under chopped UV-vis illumination (Xe-Hg Arc lamp, at 300 W output) in the same solution as (B).

The CO_2-reducing ability of the photogenerated electrons is dictated by the position of their surface quasi-Fermi level and the SC conduction band edge (Fig. S1). Therefore it is possible to *photoreduce* CO_2 *at a less negative* potential ("underpotential") relative to the thermodynamic reduction potential; the principal role of external bias potential is to augment the built-in electric field to separate the photogenerated charge carriers. This observation highlights the benefit of the PEC method over its "dark" electrochemical counterpart where usually high overpotential (thus high energy input) is needed to drive the reaction due to the kinetic constraints of CO_2 reduction.

Comparing the two curves in Fig.1A, a two-fold increase was seen in the cathodic photocurrents in the plateau region in the presence of CO_2. What is also important, the onset potential (+0.1 V vs. Ag/AgCl/3M NaCl) observed at the maximum light intensity (Fig. 1C) was several hundred mV *below* the thermodynamic potential of most of the CO_2 reduction processes, and in particular the CO_2/CH_3OH redox process (see Fig. S1) which lies at -0.41 V vs Ag/AgCl/3M NaCl at pH = 4. The pH strongly affects both the (photo)electroactivity of PANI[25] as well as the H^+ reduction (H_2-evolution) process.

Notably, to separate the intrinsic contribution of CO_2 from the more trivial pH-effect (caused by the increased H^+ concentration because of the CO_2 dissolution), the control measurement under N_2 atmosphere was recorded in a buffered solution having exactly the same pH as measured in CO_2 saturated solution (pH = 4.0±0.1, Fig. 1A). Similar comparison was performed in $NaHCO_3/CO_2$ solution (pH= 7.0± 0.1, Fig. 1B), and very similar conclusions were drawn, together with the observation of a 150 mV shift in the onset potential, which indicated the participation of H^+ ions in the CO_2 reduction. Finally, the photon flux was increased to the maximum output of the lamp (300 W), which resulted in an almost three-fold increase of the photocurrents (with a maximum of 170 μA cm^{-2}, see Fig. 1C). This proportional increase in the photoconversion rate with the photon flux suggests that carrier-recombination processes are not yet rate-limiting in the overall process.

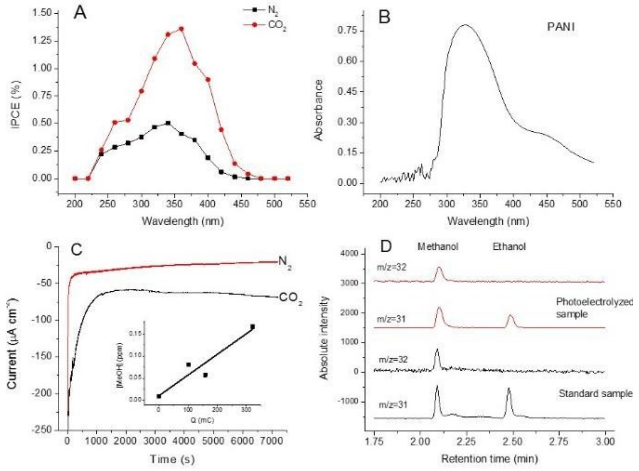

Fig. 2. A: Photoaction spectra of PANI registered at E = -0.4 V in N_2- and CO_2-saturated 0.1 M Na_2SO_4 aqueous solution. B: UV-vis spectrum of PANI registered at E = -0.4 V in CO_2-saturated 0.1 M Na_2SO_4 aqueous solution. C: Current/time profiles under continuous UV-vis light irradiation (100 W) at -0.4 V vs. Ag/AgCl/3M NaCl in a sealed two-compartment photoelectrochemical cell containing a PANI layer photocathode. Electrolyte was 0.1 M $NaHCO_3$ saturated with CO_2 (pH = 7). The inset shows the increasing methanol concentration with the transferred charge, as deduced from data shown in (D). D: GC-MS profiles registered using selective ion monitoring (SIM) for the sample after photoelectrolysis shown in Fig. 2C, as well as for a standard solution containing 0.5 ppm methanol and ethanol respectively.

To further examine the photoreduction process, photoaction spectra were measured to determine internal photon to electron conversion efficiencies (IPCE) both under N_2 and CO_2 saturation. As seen in Fig. 2A the obtained photoaction spectra perfectly corresponded to the UV-vis spectrum of PANI (Fig. 2B), recorded under identical circumstances (i.e., E = –0.4 V external bias potential). The threshold energy determined from the photoaction spectra (440 nm, 2.8 eV) nicely agreed with the bandgap energy (2.8 eV) obtained from the UV-vis spectra using the Tauc plot (not shown). Photovoltammograms were also recorded by irradiating the photocathode with simulated sunlight yielding very similar profiles both in terms of shape and absolute photocurrent values (Fig. S2).

Long term constant-potential electrolysis was performed at *E* = -0.4 V (Fig. 2C), and the formed products were analyzed using GC and GC-MS (Fig. 2D) for the gas and liquid phase, respectively. The striking difference in the stationary currents (20 µA vs. 70 µA) recorded after 2 h in the two cases suggests that the PANI layer, at least partially, maintained its PEC efficacy for the studied time period. While in the gas phase only H_2 was detected as the product in both cases (through proton reduction), methanol and ethanol (together with some minor traces of formaldehyde) were detected in the solution for CO_2-saturated samples. Importantly, no such products could be detected under N_2-saturation. In the CO_2-saturated case, it was found that 20% of the transferred charge (Faradaic efficiency) accounts for H_2 formation, while the rest is responsible for the alcohol formation with an approximately 2:1 methanol/ethanol molar ratio (~43% and ~20%) indicating that the measured photocurrent is related to the formation of the listed products.

During the long term photoelectrolysis, an initial decrease in the photocurrents was always observed (see also in Fig. 2C). At the same time, the intrinsic *electro*activity of the PANI films did not change significantly (as probed by cyclic voltammetry before and after photoelectrolysis, see Fig. S3). This fact confirms that no a molecular or supramolecular degradation is the process behind the decrease of the PEC performance. Scanning electron microscopic images (SEM) furnished insights on this peculiar phenomenon, namely that the decrease in the PEC activity is predominantly rooted in the melting of the polymer (Fig. S4). Melting of the PANI film causes a decrease in the surface area, thus the majority of the photoactive material becomes inaccessible for the CO_2 saturated solution. Such light-induced melting was reported earlier for PANI[26], and in our case the local heating, induced by charge carrier recombination, is responsible for this phenomenon.

To further probe the factors behind the PEC activity, similar data as in Fig. 1 are contained in Fig. S5 for PPy and poly(3,4-ethylenedioxythiophene) (PEDOT); these show that both these conducting polymers afford only negligible photoeffects from CO_2 reduction. The conduction band edge positions of these polymers were located negative enough to reduce CO_2 (Fig. S1). Therefore the lack of photoactivity clearly does not reside with reduced driving force for photoinduced electron transfer in these other cases relative to PANI. In other words, factor(s) beyond thermodynamics must control the rather unique ability of PANI to photoelectroreduce CO_2. With the notion that the chemical environment of the *N*-atom in PANI must be of special importance, similar experiments (as in Fig. 1) were carried out with poly(N-methylaniline) (PNMANI). The only difference here from PANI is the lack of *H*-substituent on the *N*-atom in the conjugated structure, the hydrogen being substituted by a methyl group. Importantly, the enhanced PEC behavior seems to be unique to PANI, because no such increase can be seen for its $–CH_3$ derivative (Fig. S5); clearly this small structural difference exerts a huge impact on CO_2 photoreduction efficacy.

Figure 3A compares three adsorption /desorption sequences for the above-discussed polymers on supporting gold electrodes, as derived from quartz crystal microgravimetry (QCM) measurements. The largest adsorbed amounts were detected for PANI, and also somewhat surprisingly, for PPy. In addition, careful comparison of the desorption portion of these data revealed striking differences: while for PNMANI, the mass decreased rapidly upon N_2 purge (10-15 s), in the case of PANI it took 300 s to reach the original mass value. Note that all these polymer films were electrodeposited with identical charge density; therefore their thickness was also very similar. Consequently we have to assume that there is specific chemical interaction between PANI (and PPy) and the CO_2 molecules which clearly does not exist for PEDOT and PNMANI beyond simple physisorption.

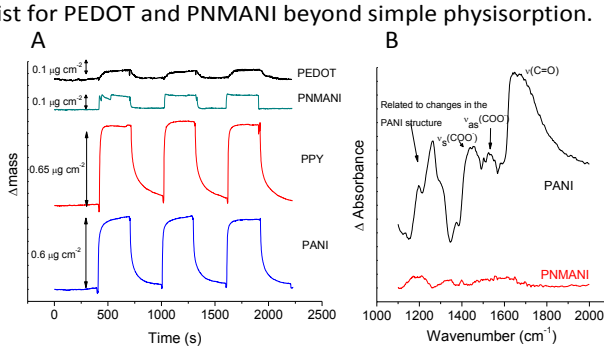

Fig. 3. A: Subsequent mass changes upon CO_2 and N_2 exposure for the various conducting polymer films, as registered by QCM. B: Changes in the FT-IR spectra of PANI and PNMANI upon exposure to CO_2 for 5 min; the background was the respective polymer pre-treated in He in both cases (refer to text).

To shed further light on the underlying surface chemistry, a series of diffuse reflectance FT-IR spectra were recorded for both PANI and PMANI, both before and after being in contact with CO_2 (Fig. 3B). The difference is striking: while a set of new vibrations are visible for PANI, there is no change for PNMANI (Fig. 3B). The changes observed for PANI are the superposition of the alteration of the original PANI spectrum (because of protonation, see Scheme 1)[27] and the bands related to the chemisorbed CO_2. The appearance of the ν(C=O) at 1680 cm^{-1} (in carbamic acid) as well as the $\nu_{as}(COO^-)$ and $\nu_s(COO^-)$ vibrations at around 1530 cm^{-1} and 1450 cm^{-1} respectively[28,29] confirms the formation of carbamic acid and carbamate (see Scheme 1) as reported for primary and secondary amine-containing (non-conductive) polymers[29] and PANI-based composite materials[30-31]. Importantly, the vibrations related to physisorbed CO_2 are of very similar intensity in the two cases.

Taking all the findings from this study together as a whole, the following reaction scheme is suggested for the PEC reduction of CO_2 by PANI. The formation of protonated PANI rationalizes the observed color change upon CO_2 adsorption and is a necessary but not sufficient criterion. Adsorption of CO_2, while important, is also not enough as seen by the example of PPy. The polymer band edge positions (see Fig. S1) are critical in at least two respects: (i) The CB edge (LUMO band position) of the conducting polymer has to be negative enough for the photogenerated electrons to reduce CO_2; (ii) The VB edge (HOMO band position) has to be positive enough, to make the conducting polymer behave as a SC (rather than as a semi-metal) at the potential where the PEC experiment is performed. In the latter case, the polymer electroactivity would dominate, as exemplified here by the PPy case (Fig. S6).

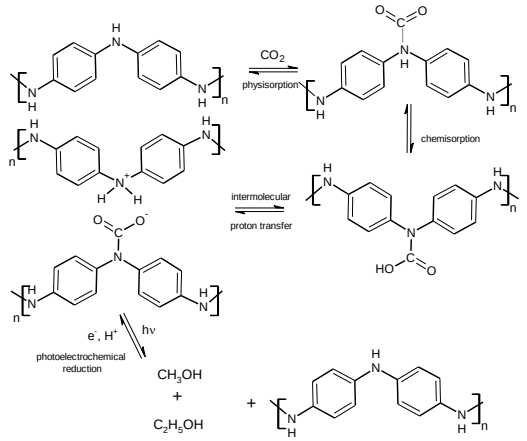

Scheme 1. Possible mechanistic pathway for CO_2 adsorption and photoelectroreduction on PANI.

Conclusions

In summary, the present study underlines the rather different prerequisites for a given conducting polymer to behave as an electrocatalyst (as demonstrated by previous authors in the literature) or as a photocathode capable of reducing CO_2 as demonstrated in this study. In a PEC process designed to drive a given reaction thermodynamically uphill (as in the CO_2 reduction case), photoexcitation of the cathode material initially serves to "pump" the species against the free-energy gradient. The reversible chemical interaction between the PANI surface and CO_2 then fulfills the *catalytic role where multiple electrons are stored* and *transferred.* The above-described chemisorption plays a key role in protonating/binding CO_2, as well as possibly the intermediate products in the initial reduction step, thereby increasing their residence time on the electrode surface.

It is also worth noting that PANI was seen here to be able to photoreduce CO_2 in the absence of a co-catalyst. In this sense, the choice of PANI as a candidate photocathode material has practical significance in that aniline is among the commodity chemicals produced in the largest amounts globally (well over 4 million tons/year). Consequently, large quantities are available at an economically viable price (about 2 USD/kg) (vs. Si-based photoelectrodes). In addition, PANI can be obtained by simple chemical or electrochemical polymerization. The proof-of-concept data in this Communication were collected for PANI films under unoptimized conditions. PANI films with high surface area in a nanocomposite configuration may result in even higher photoconversion rates and improved stability. For example, depositing PANI on a carbon nanotube network (see Fig. S7 for SEM images)[32] further enhances the process efficiency through better charge separation/transport, as shown in Fig. S8. With identical PANI amount, strikingly higher photocurrents (up to 0.5 mA cm^{-2}) were obtained, underlining the promise to practically exploit the proof-of-concept presented herein.

Notes and references

1 N. Lewis and D. Nocera, *Proc. Natl. Acad. Sci.*, 2006, **104**, 15729–15735.
2 A. M. Appel, J. E. Bercaw, A. B. Bocarsly, H. Dobbek, D. L. Dubois, M. Dupuis, J. G. Ferry, E. Fujita, R. Hille, P. J. A. Kenis, C. a Kerfeld, R. H. Morris, C. H. F. Peden, A. R. Portis, S. W. Ragsdale, T. B. Rauchfuss, J. N. H. Reek, L. C. Seefeldt, R. K. Thauer and G. L. Waldrop, *Chem. Rev.*, 2013, **113**, 6621–6658.
3 K. Rajeshwar, *J. Phys. Chem. Lett.*, 2011, **2**, 1301–1309.
4 D. J. Boston, K. L. Huang, N. R. de Tacconi, N. Myung, F. M. MacDonnell and K. Rajeshwar, in *Photoelectrochemical Water Splitting: Materials, Processes and Architectures*, 2013, 289–332.
5 K. Sivula, *J. Phys. Chem. Lett.*, 2015, **6**, 1624–1633.
6 J.-W. Jang, S. Cho, G. Magesh, Y. J. Jang, J. Y. Kim, W. Y. Kim, J. K. Seo, S. Kim, K.-H. Lee and J. S. Lee, *Angew. Chemie Int. Ed.*, 2014, **53**, 5852–5857.
7 U. Kang, S. K. Choi, D. J. Ham, S. M. Ji, W. Choi, D. S. Han, A. A. Wahab and H. Park, *Energy Environ. Sci.*, 2015, **8**, 2638–2643.
8 M. Halmann, *Nature*, 1978, **275**, 115–116.
9 J. Bockris and J. C. Wass, *Mater. Chem. Phys.*, 1989, **22**, 249–280.
10 B. Kumar, M. Llorente, J. Froehlich, T. Dang, A. Sathrum and C. P. Kubiak, *Annu. Rev. Phys. Chem.*, 2012, **63**, 541–69.
11 E. Barton, D. M. Rampulla and A. B. Bocarsly, *J. Am. Chem. Soc.*, 2008, **130**, 6342–6344.
12 G. Ghadimkhani, N. R. de Tacconi, W. Chanmanee, C. Janaky and K. Rajeshwar, *Chem. Commun.*, 2013, **49**, 1297–1299.
13 Y. Oh and X. Hu, *Chem. Soc. Rev.*, 2013, 2253–2261.
14 A. Goeppert, M. Czaun, G. K. Surya Prakash and G. A. Olah, *Energy Environ. Sci.*, 2012, **5**, 7833.
15 J. Wang, L. Huang, R. Yang, Z. Zhang, J. Wu, Y. Gao, Q. Wang, D. O'Hare and Z. Zhong, *Energy Environ. Sci.*, 2014, **7**, 3478–3518.
16 Y. Xie, T.-T. Wang, X.-H. Liu, K. Zou and W.-Q. Deng, *Nat. Commun.*, 2013, **4**, 1960.
17 A. Zhang, W. Zhang, J. Lu, G. G. Wallace and J. Chen, *Electrochem. Solid State Lett.*, 2009, **12**, E17–E19.
18 R. D. L. Smith and P. G. Pickup, *Electrochem. Commun.*, 2010, **12**, 1749–1751.
19 B. Aurian-Blajeni, I. Taniguchi and J. Bockris, *J. Electroanal. Chem.*, 1983, **149**, 291–293.
20 D. Won, J. Chung, S. Park, E. Kim and S. Woo, *J. Mater. Chem. A*, 2015, **3**, 1089–1095.
21 A. Guerrero, M. Haro, S. Bellani, M. R. Antognazza, L. Meda, S. Gimenez and J. Bisquert, *Energy Environ. Sci.*, 2014, **7**, 3666–3673.
22 P. Bornoz, M. S. Prevot, X. Yu, N. Guijarro, K. Sivula, P. Bornoz, M. S. Prévot, X. Yu, N. Guijarro and K. Sivula, *J. Am. Chem. Soc.*, 2015, **137**, 15338–15341.
23 E. B. Cole, P. S. Lakkaraju, D. M. Rampulla, A. J. Morris, E. Abelev and A. B. Bocarsly, *J. Am. Chem. Soc.*, 2010, **132**, 11539–11551.
24 K. Rajeshwar, in *Electron Transfer in Chemistry*, ed. V. Balzani, Wiley- VCH, Weinheim, 2001.
25 P. Kilmartin and G. Wright, *Electrochim. Acta*, 1996, **41**, 1677–1687.
26 J. X. Huang and R. B. Kaner, *Nat. Mater.*, 2004, **3**, 783–786.
27 S. Quillard, G. Louran, S. Lefrant and A. G. MacDiarmid, *Phys. Rev. B*, 1994, **50**, 496–508.
28 A. Danon, P. Stair and E. Weitz, *J. Phys. Chem. C*, 2011, **115**, 11540–11549.
29 W. C. Wilfong, C. S. Srikanth and S. S. C. Chuang, *ACS Appl. Mater. Interfaces*, 2014, **6**, 13617–13626.
30 A. K. Mishra, S. Ramaprabhu, *J Mater Chem*, 2012, **22**, 3708-3712
31 S. Khalili, B. Khoshandam, M. Jahanshahi, *RSC Advances,* 2016, **6**, 35692-35704
32 C. Janáky and K. Rajeshwar, *Prog. Polym. Sci.*, 2015, **43**, 96–135.